ELSEVIER

Biophysical Chemistry 125 (2007) 24–31

Biophysical Chemistry

http://www.elsevier.com/locate/biophyschem

Photophysics of ANS III: Circular dichroism of ANS and anilinonaphthalene in I-FABP

William Kirk *, Elena Klimtchuk

Mayo Clinic School of Medicine Rochester Minn, 55905, United States

Received 18 January 2006; received in revised form 26 July 2006; accepted 31 July 2006
Available online 12 August 2006

Abstract

We investigate the circular dichroism of the I-FABP system with the ligands ANS (1,8-anilinonaphthalene sulfonate) and AnN (anilinonaphthalene) as previously reported in our earlier publications in the series (referred to as I and II here) on ANS photophysics. We employ our semi-empirical calculated spectral functions (from II) to compute the actual CD spectra, without any additional assumptions or data except what we have previously presented with respect to binding geometry (in I). The common mechanisms fail to produce the observed spectra. However, we identify a novel mechanism of induced CD activity, which does succeed. This new mechanism also suggests how it is that near UV CD can often show extreme sensitivity to local 'order' effects.
Published by Elsevier B.V.

In order to provide a test for the ANS and AnN spectra we composed in our previous report on ANS photophysics, (referred to as II), in this report, we construct the expected near UV circular dichroism spectra for both compounds bound to intestinal fatty acid binding protein (I-FABP). We find that both the coupled dipole and the 'intrinsic' magnetic dipole contributions are insufficient to recover the observed CD signal. We surmise therefore the existence of a novel mechanism which does account for the observed results in both ANS and AnN. The new mechanism we uncover here dominates the CD in the near UV region in the I-FABP/ANS, I-FABP/AnN system. It fairly promises not only to be a major contributor to the CD in related systems, but also to make a large contribution in induced CD spectra in protein/ligand systems generally, especially in those cases wherein the near UV signal seems to be a reporter of a 'local order' parameter. Briefly, the new mechanism consists of a two-quantum (resonant) effect wherein a transition dipole on one residue creates a local electric field gradient, which in turn excites a quadrupole moment transition on a nearby second residue. The interference between the induced field gradient/quadrupole moment and the dipole transition moment of the second residue causes CD activity.

In the previous report (II), we examined the nature of the transitions in the near UV for AnN and for ANS. We concluded that the transitions in the 250–290 nm region were of two kinds: one originating as an 'anilino'-type (recalling that of aniline itself) and one originating as a charge-transfer-type. These became substantially mixed, because of spatial and energy overlap. The new transitions were simply labeled 'A' and 'B', and their respective energies and oscillator strengths were determined with the aid of an assumed set of dipole moments. We propose to calculate, given no more information than we already have regarding the I-FABP protein structure with ANS present, together with the dipole moments and charge distribution associated with the tryptophan ^{1}L and ^{1}L transitions and our previously determined 'A' and 'B' transitions, the expected circular dichroism activity in this region for the ANS(AnN)/I-FABP system.

Initially, one may wonder how it is that ANS has any CD activity at all—given that there is no chiral center in the ANS ligand. The reason is that the environment of the ANS bound to I-FABP is not isotropic, that mirror image symmetry does *not* occur in the protein-ANS complex. The conformation of the two rings of ANS or AnN are possibly fixed relative to the background molecular frame of the protein in which it resides, the 'mirror image' conformer would rest in the same pocket only if one or the other ring is capable of some 5Å or more freedom of movement.

* Corresponding author.
E-mail address: kirk.william@mayo.edu (W. Kirk).

0301-4622/$ - see front matter. Published by Elsevier B.V.
doi:10.1016/j.bpc.2006.07.018

Table 1

	N	C2	C3	C4	C5	C6	C7	C8	C9
^1L_a	−0.302	−0.677	0.554	0.847	−0.478	0.715	−0.676	0.554	−0.537
^1L_b	−0.547	0.570	−0.150	−0.293	−0.156	−0.200	−0.395	0.620	0.542

Values are in 'Debye units', i.e. 10^{-10} esu, or 1/4.8 of an electron charge.

In addition to conformational restraint, a local 'order parameter' may be manifest in the local *field*. Power and Thirunamachandran [1] have discussed the origin of CD effects in ordered systems (they refer to crystals) wherein electric multipole fields of different parity produce large Cotton effects. These, however, are averaged out over random orientations. Nonetheless, an electric multipole active residue of a protein may experience a local field which is anisotropic, which does not average out even when the protein itself is randomly oriented throughout the sample, because the source of that additional field is also local.

1. Theory and calculations

1.1. Circular dichroism

There are two well-studied mechanisms for generating CD in typical chromophores: the 'intrinsic magnetic dipole' mechanism and the 'distributed dipole' mechanism. CD is generated by considering the cross term in the *complex* squared matrix element for interaction with radiation [1,2]

$$\langle \boldsymbol{\mu} \rangle^2 = \langle \boldsymbol{\mu}_{\mathrm{el}} + i\mathbf{m} \rangle^2 \tag{1a}$$

The cross term is then:

$$2i\langle \boldsymbol{\mu}_{\mathrm{el}} \rangle \cdot \langle \mathbf{m} \rangle, \text{ where } \langle \mathbf{m} \rangle = (e/M_{\mathrm{el}}c)\mathbf{r} \times \mathbf{p} \tag{1b}$$

for the intrinsic magnetic dipole term, i.e. if the transition involves a change in orbital angular momentum (or else spin, but we assume we are dealing here entirely with singlet states, so there is no unpaired spin). M_{el} is the electron mass and e is the electron charge. A twisted internal charge transfer mechanism would have an angular momentum component, so we include a term for this possibility, since the 'A' exciton we found for ANS itself in II has an imaginary component—strongly suggesting there is indeed 'twist' to the transition.

The 'orbital angular momentum' term $\mathbf{r}\times\mathbf{p}$ is quantized in units of $\hbar$, thus we calculate the term $\hbar(e/M_{\mathrm{e1}}c)(8\pi/3h^2)\hbar N_0/1000c\ln 10$.

Given the $\mathbf{f}(A,\mathrm{new})$, etc. eigenfunctions (see below), we have:

$$8.094\boldsymbol{\mu}(\mathrm{Debye})\varpi\ (\mathrm{cm}^{-1})\mathbf{f}\ (\mathrm{cm}^{-1})^{-1} = \Delta\varepsilon\ (\mathrm{M}^{-1}\ \mathrm{cm}^{-1}) \tag{2}$$

for the CD spectrum contributed (as the difference 'left–right' in molar extinction, $\Delta\varepsilon$; with z the direction of propagation and a right handed coordinate system, the rotation "$x+iy$" is 'right handed') by the orbital magnetic moment for each 'new' exciton, multiplied by the mixing coefficients for the original A exciton into each new exciton as calculated below. In formula (2), ϖ (cm^{-1}) is the wavenumber of each point in the spectrum. We display the units of each quantity we employ appropriate to the numerical coefficient given at the front of the expression.

For the distributed magnetic dipole–electric dipole contribution, we calculate $-\mathbf{R}_{12}\cdot\propto_1\times\propto_2$ where $\mathbf{R}_{12}$ is the separation vector between the two relevant (coupled) transition dipoles. After evaluation of the physical constants, we obtain:

$$1.37\times10^{-5}[-\mathbf{R}_{12}\cdot\propto_1\times\propto_2]\ (\mathrm{Debye}^2\ -{}^{\circ}\mathrm{A})\varpi^2\ (\mathrm{cm}^{-2})\mathbf{f} \times(\mathrm{cm}^{-1})^{-1} = \Delta\varepsilon \tag{3}$$

for this CD spectral contribution. All these values are evaluated into units of $\Delta\varepsilon$ (the molar extinction coefficient in $\mathrm{M}^{-1}\ \mathrm{cm}^{-1}$). The values for the $-\mathbf{R}_{12}\cdot\boldsymbol{\mu}_1\times\boldsymbol{\mu}_2$ term are collected in Table 2.

There is however a more novel mechanism, which we investigate now. A transition dipole at one site is imagined to be in near resonance with a transition at another site. In order to provide a CD signal, one needs an odd symmetry over three spatial axes to arise, and one effective way is to regard the second transition as a quadrupole. The first transition dipole generates a field gradient which excites the second transition.

Thus, the dipole at the first site or $\propto_1$ interacts with the quadrupole moment $\mathbf{Q}_{\mathrm{ab}}$ at the second site with an energy H_{int}:

$$H_{\mathrm{int}} = (3/r_{p,Q}^4)[-5\mathbf{nn}(\boldsymbol{\mu}_1\cdot\mathbf{n}) + \mathbf{n}\boldsymbol{\mu}_1 + 1(\boldsymbol{\mu}_1\cdot\mathbf{n})] : \mathbf{Q}_{\mathrm{ab}} = \mathbf{G}:\mathbf{Q} \tag{4}$$

where the $\mathbf{n}$ are normed displacement vectors between the two moments, and the tensor product notation is employed (with $\mathbf{G}$ standing for gradient of the dipole electric field created by the μ_1 dipole and I for the identity matrix). The double contraction ":" stands for the summation $\sum_i\sum_j G_{ij}Q_{ij}$, i.e. both indices i and $j\in(x,y,z)$ must agree between the two operators. The quadrupole moment is found from the graphs produced by Callis [3], and given in Table 1.

The new CD term [2] is then

$$\mathbf{A}\{x,y,z\}[(\boldsymbol{\mu}_1\cdot E(t))/(E-h\nu)]\mathbf{G}:\mathbf{Q}(\boldsymbol{\mu}_2\cdot E(t)) \tag{5a}$$

because the first transition acts as an intermediate state (coupled by $\mathbf{G}$:$\mathbf{Q}$) to the second transition. In (5a), $\mathbf{A}$ is an antisymmetrizer and $E(t)$ is the impinging electric field vector. The two-quantum formalism leads to the energy denominator [4], which, when considered as the Fourier transform of a time dependent interaction [5], leads to the energy distribution of the exciton at '1', or i.e. the normalized spectrum $\mathbf{f}_1(\nu)$, as in our previous report (II). The antisymmetrizer ensures that mirror image and inversion symmetry will be removed from the signal. We then write the CD active interaction as:

$$\mathbf{f}_1(\nu)\boldsymbol{\mu}_{1i}(GQ)_{ij}\boldsymbol{\mu}_{2k}\varepsilon_{i,j,k} \tag{5b}$$

where $\varepsilon_{ijk}=+1$ if i,j,k are an even permutation of x,y,z, -1 if an odd permutation, and zero if any index is repeated. We find:

$$552.9\mathbf{f}_1\ (\mathrm{cm}^{-1})^{-1}[\boldsymbol{\mu}_{1i}(GQ)_{ij}\boldsymbol{\mu}_{2k}\quad \varepsilon_{i,j,k}\ (\mathrm{Debye}^4\circ\mathrm{A}^{-3})]\varpi \times(\mathrm{cm}^{-1})\mathbf{f}_2\ (\mathrm{cm}^{-1})^{-1}=\Delta\varepsilon \tag{5c}$$

for the new term in the CD spectrum.

1.2. Exciton (re)coupling

We recap some of our formalism from II: An electronic ground state $|a\rangle$ is mapped to the excited state $|b\rangle$ via the paired annihilation/creation operators **a** and $\mathbf{b}^\dagger$; hence, we write $\mathbf{b}^\dagger\mathbf{a}$ as the *exciton* creation operator $\mathbf{A}^\dagger$. This now implies an exciton *state* $|A\rangle=\langle b|a\rangle$, hence also the *spectrum* (to be exact, the observed spectrum $I(\nu)$ divided by ν and the square of the transition dipole moment) is given by $\mathbf{f}(A)=\|A\|^2=\langle A|A\rangle=\langle b|a\rangle\langle a|b\rangle$, and is, as expected, a probability distribution function. All this formalism was required to justify the subsequent orthogonalization and principle axis transformations performed on the 'square root' of the spectrum, as if it were an ordinary quantum wavevector. The exciton formalism will be used again in a similar way to mix the 'A' and 'B' spectra of ANS (and AnN) with the L_a and L_b spectra of tryptophan—specifically *trp*-82 of FABP.

We first generate a representation of these transitions, as in Table 1: We also generate the dipole–dipole interaction matrix element between the dipoles of each transition, from the known (previously reported) values of the dipole moments of AnN and ANS:

$$H_{\mathrm{int}}=-[\boldsymbol{\mu}_1\cdot\boldsymbol{\mu}_2-3\boldsymbol{\mu}_1\cdot\mathbf{u}_{12}\boldsymbol{\mu}_2\cdot\mathbf{u}_{12}]/\in r_{12}^3 \tag{6}$$

Here $\mathbf{u}_{12}$ is the normed separation vector of the two electric dipole moments $\boldsymbol{\mu}_1$ and $\boldsymbol{\mu}_2$. The term $\in$ is the high-frequency dielectric constant—we employ a value of 2.1 for a hydrophobic site, although a different choice would be the square of the refractive index at the optical wavelengths of interest. That value would be $(1.37)^2$ or 1.88. The difference does not substantially affect the results. These matrix elements are collected in Table 2.

Since the basis eigenvectors 'A' and 'B' have no interaction, and likewise the basis eigenvectors L_a and L_b of *trp* are not expected to have any interaction either, we find the 'eigenvalues'—in our case, the distribution functions (which are normalized to 1.00 when integrated over energy) are multiplied by the energy and integrated over energy, from the eigenvalues of the matrix, **M**1=

$$\begin{vmatrix} \int \mathbf{f}(\mathrm{A})E\mathrm{d}E & \langle A|\mathrm{H_{int}}|\mathrm{L_a}\rangle & \langle A|\mathrm{H_{int}}|\mathrm{L_b}\rangle \\ |\langle A|\mathrm{H_{int}}|\mathrm{L_a}> & \int \mathbf{f}(\mathrm{L_a})E\mathrm{d}E & 0 \\ |<A|\mathrm{H_{int}}|\mathrm{L_b}> & 0 & \int \mathbf{f}(\mathrm{L_b})E\mathrm{d}E \end{vmatrix} \tag{7a}$$

which for convenience we rewrite (*cf.* Appendix A):

$$\begin{vmatrix} H_{\mathrm{A}} & H_{\mathrm{Aa}} & H_{\mathrm{Ab}} \\ |H_{\mathrm{Aa}} & H_{\mathrm{a}} & 0 \\ |H_{\mathrm{Ab}} & 0 & H_{\mathrm{b}} \end{vmatrix} = \mathbf{M}2 \tag{7b}$$

and a similar matrix is employed for the 'B' transitions. The solution of **M**2 for the eigenvalues as a function of wavenumber–i.e. the distribution of energies–is discussed in Appendix A. The

Table 2
Matrix elements for A,B:L_a,L_b dipole interaction (cm^{-1})

	A:		B	
	L_a	L_b	L_a	L_b
ANS				
α	−181	+168	−367	−14.0
β	35.4	−14.5	−97.1	−54.0
AnN				
α	−282	288	−265	−148
β	68.1	−20.4	−133	−47.0

Electric-distributed magnetic dipole CD term ($\propto\cdot R_{12}\times\propto_2$) ($\mathrm{D}^2$-Å)

	A:		B	
	L_a	L_b	L_a	L_b
ANS				
α	−19.3	2.35	9.55	−2.92
β	35.7	8.63	15.8	−3.30
AnN				
α	−33.7	4.25	5.52	23.2
β	59.7	15.0	−11.2	1.46

α and β refer to the two conformers, of occupancy 65% and 35% found for the ANS-I-FABP complex for *trp*-82, as in the previous report I. 'A' and 'B' refer to coupling to the two transitions of AnN or ANS labeled as such in II, L_a and L_b refer to the transitions of indole.

eigenvectors, however, are different from these energy distributions. They are given by the mixing coefficients for the *real space transition densities* underlying the spectral distributions. And these coefficients are used to compose the CD signal.

The CD interaction, as we said in (7a), is the cross-term of a squared matrix element. If the 'new' mixed excitons are written as linear combinations of the underlying basis excitons (the unaltered original excitons for each transition, before perturbation causes them to be mixed), as e.g.

$$|A,new\rangle=c_{11}|A\rangle+c_{12}|a\rangle+c_{13}|b\rangle \tag{8a}$$

and similar expansions for the other transitions; then the CD contribution (from transition '1') can be written in terms of the separate CD contributions of the original basis excitons as:

$$\begin{aligned}&\langle c_{11}A+c_{12}a+c_{13}b|\boldsymbol{\mu}-i\mathbf{m}|0\rangle\langle 0|\boldsymbol{\mu}+i\mathbf{m}|c_{11}A+c_{12}a+c_{13}b\rangle\\ &\quad-\text{Right hand terms}=\Delta\varepsilon(\text{left}-\text{right})=4c_{11}c_{12}\langle A|\boldsymbol{\mu}\cdot\mathbf{m}|a\rangle\\ &\quad+4c_{11}c_{13}\langle A|\boldsymbol{\mu}\cdot\mathbf{m}|b\rangle\end{aligned} \tag{8b}$$

These cross terms $\langle A|\boldsymbol{\mu}\cdot\mathbf{m}|a\rangle$, $\langle A|\boldsymbol{\mu}\cdot\mathbf{m}|b\rangle$ (and similarly, those for the transition 'B' for AnN and ANS as well) are calculated from the formulas (2) and (3) above and presented in Table 2. These mixing coefficients, c_{11}, c_{12}, etc., can be looked upon as angles of unitary rotation matrices (cf. II), which leads to the following description of the eigenvectors in terms of the basis vectors:

$$|A\rangle\mathrm{new}=|A\rangle\cos\chi\cos\phi-|a\rangle\sin\chi\cos\phi-|b\rangle\sin\phi$$

$$|a\rangle\mathrm{new}=|A\rangle\sin\chi+|a\rangle\cos\chi$$

$$|b\rangle\mathrm{new}=A\rangle\cos\chi\sin\phi-|a\rangle\sin\chi\sin\phi+b\rangle\cos\phi \tag{9a, b, c}$$

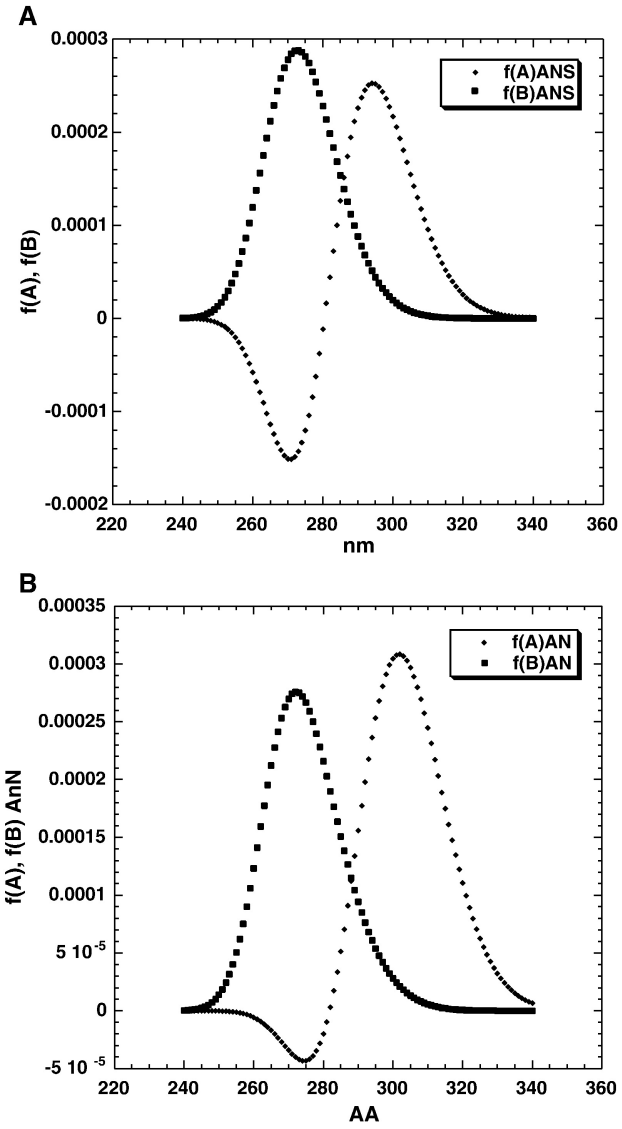

Fig. 1. Exciton distributions for the 'A' and 'B' transitions of (a) ANS and (b) AnN. These are reproduced in II. They are normalized such that $\int|f(\varpi)|d\varpi = 1.00$ with ϖ in wavenumbers (cm^{-1}). Note that they are plotted, however, in the nanometer scale.

comparing these equations to the eigenvalue equations (for $\mathbf{f}(A)$, new, $\mathbf{f}(a)$,new and $\mathbf{f}(b)$,new), we obtain the following set:

$$\sin^2\chi = [\mathbf{f}(a,\text{new}) - \mathbf{f}(a)]/[\mathbf{f}(A) - \mathbf{f}(a)]$$

$$\cos^2\phi = [\mathbf{f}(A,\text{new}) - \mathbf{f}(b)]/[\mathbf{f}(a) - \mathbf{f}(A))\sin^2\chi + \mathbf{f}(A) - \mathbf{f}(b)]$$

$$\sin^2\phi = [\mathbf{f}(b,\text{new}) - \mathbf{f}(b)\cos^2\phi]/(\mathbf{f}(a) - \mathbf{f}(Aa))\sin^2\chi + \mathbf{f}(A)] \qquad (10a,b,c)$$

where $\mathbf{f}(A,\text{new})$, $\mathbf{f}(a,\text{new})$, $\mathbf{f}(b,\text{new})$ are the 'new' eigenvalue distributions for the original 'A', L_a and L_b transitions we obtained from the matrix $\mathbf{M}$ as described in Appendix A.

It should be noted that these terms in χ and ϕ are simply coefficients at each point in wavenumber space, though originally they referred to real trigonometric functions—for instance, at some wavenumbers, the value found for $\sin^2\chi$ can be >1, or even negative. At these points, we can say that they represent 'improper' rotations. Thus, in the language we used above in (8a) and (8b), the coefficients c_{11}, c_{12} and c_{13} are represented by $\cos\chi\cos\phi$, $-\sin\chi\cos\phi$ and $-\sin\phi$, respectively, and so on for the other coefficients (cf. (9a,b,c)).

2. Results and discussion

Fig. 1 displays the original exciton spectra for the 'A' and 'B' spectra of ANS and AnN, while Fig. 2 shows the original indole L_a and L_b spectra we employed. Fig. 3 shows the four eigenspectra for the excitons after 'mixing' them in the I-FABP-AnN bound system. Calculated values for the CD from the two conformers of the bound state (cf. I), namely α and β are included in Table 1.

The total CD calculated for the terms of [2,3] are shown for ANS and AnN in Fig. 4, and compared with the CD contribution from term [5] there. It can be seen that the term in [5], the 'GQ' term, dominates the CD as calculated. Comparison between Fig. 5, the actual experimental CD plot for ANS, Fig. 7, the observed CD for AnN, and Fig. 6, the calculated CD (summed for all contributions) for ANS and AnN, shows that the calculated CD for the one interaction with *trp*-82 seems to capture the bulk of the CD signal actually obtained.

3. Comparisons of near UV CD: I-FABP mutants and ANS analogs

For ANS, it is clear from Fig. 5 that the presence of *trp*-82 in the W6Y mutant enhances the ANS CD signal already present in the double mutant W6YW82Y—which signal is essentially the same as in the W82Y mutant. Yet the wild type protein has a CD even higher than that in the W6Ymutant. There is little enhancement due to the presence of *trp*-6 relative to the double

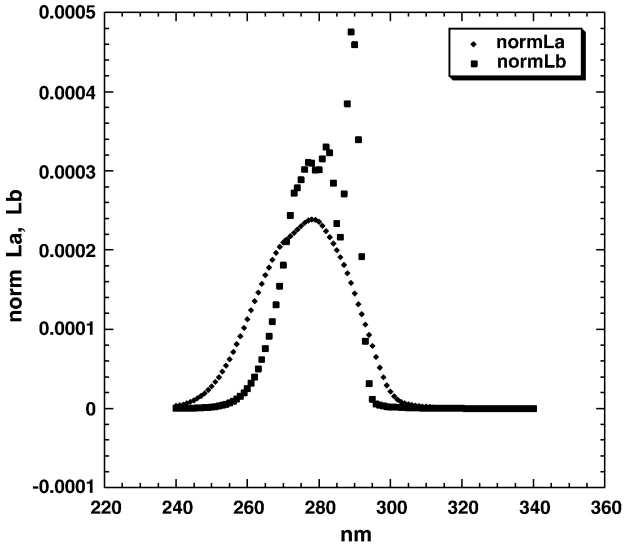

Fig. 2. The normalized distributions for ^1L_a and ^1L_b transitions of tryptophan, normalized as in Fig. 1. The molar extinction curves would be given by this distribution multiplied by ϖ, by the square of the transition dipole moment and by the numerical factor 109.8.

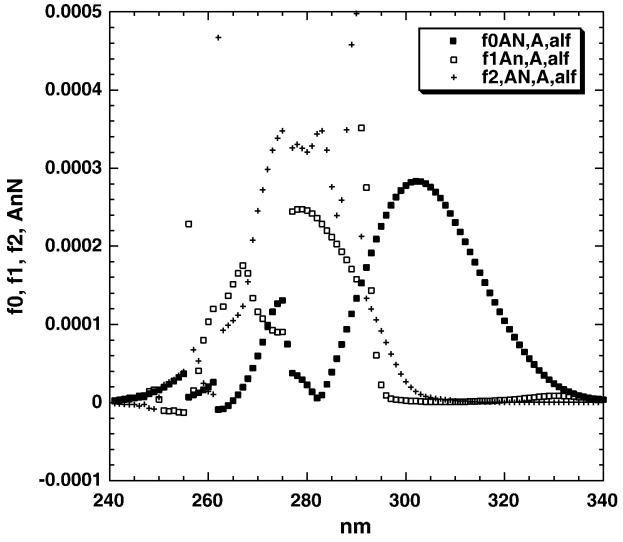

Fig. 3. Spectral (eigenvalue) distributions of AnN 'A' spectrum plus trp L_a and L_b after recoupling in **M**1. These were the found values for the α or major, conformer of *trp*-82 as determined by nmr, and previously described (in I).

mutant. Thus, while some small coupling to *trp*-6 of the above sort as we calculated may enhance the CD as observed in the wild type protein complex, the further CD enhancement in the wild type complex, relative to W6Y may well be due to increased 'stiffness' of the binding site in the wt. protein. While our new mechanism does seem to generate the observed CD signal for ANS and AnN in theW6Ymutant–and we calculated *only* the involvement for *trp*-82–the question remains: 'why is the CD signal for the W82Y mutant or the double mutant W6YW82Y still substantial when these proteins lack *trp*-82 altogether?" The only reasonable explanation would seem to be that *tyr* at site 82 may also have a significant quadrupole moment which can couple to the ANS transitions, albeit with about half the strength of *trp*. Yet this explanation is not completely satisfying: the W82Y mutant has *no* CD activity in the 260–290 nm *or* 320–380 nm region with AnN (in Fig. 7), as if removing the *trp* residue at 82 does indeed abolish the signal. Once again the naphthalene *sulfonate* seems to be playing an important role. The lack of *tyr* contribution may have something to do with freedom of ring rotational movement of the *tyr*-82 in the AnN case which does not occur in the ANS case.

In comparisons with other proteins, although ALBP (adipocyte lipid binding protein—data not shown) has some CD intensity in the 'A' region as well, it is nowhere near as strong as I-FABP. This is not surprising, since there is an appreciably more capacious cavity in the ALBP case—the rings of ANS are probably not as conformationally constrained, and moreover the nearby trp residue may have more conformational freedom than in I-FABP as well. If in ALBP the trp residue has a dominant conformer equivalent to the β conformer present in I-FABP, then the CD signal could be calculated to be as weak as that of the β contribution, which correctly yields the observed magnitude of the effect.

Similarly, while apomyoglobin (data not shown) has an even more hydrophobic insertion site for ANS than I-FABP, there is probably no selection for one sense of ring conformer over another within the planar binding pocket for ANS, which coincides with that of the heme group in *holo*myoglobin [6]. Indeed, the ANS could insert in either mirror image configuration, and hence there is very little observed CD activity from bound ANS.

In the near visible range, from 330 to 400 nm ANS, and to a slightly lesser extent AnN have some CD activity, though much less than in the near UV region (Figs. 5 and 7). There are no other absorbing dipoles in this energy range, and there is a close correlation of the sign and intensity of the CD in this region to that in the 260–290 nm region for ANS between the various mutants, while the correlation is reversed in sign for AnN (but AnN and ANS agree in sign and are similar in strength). The

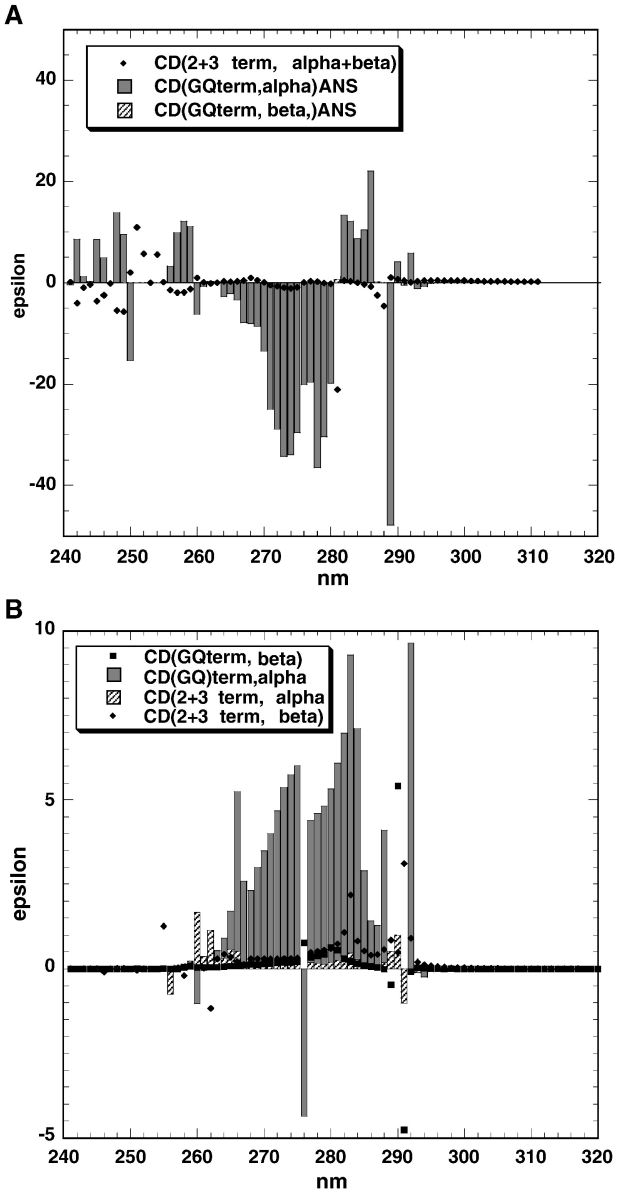

Fig. 4. (A) The sum of the terms from Eqs. (2) and (3) (the coupled dipole and the magnetic dipole terms) for ANS in (♦) for both conformers; the contribution of Eqs. (5a) (5b) (5c) to the CD, each conformer separately shown (i.e. the two-quantum 'GQ' terms = shaded bars). In (B), the comparable terms for AnN. Units are differential molar extinction (left minus right) or Δ(epsilon).

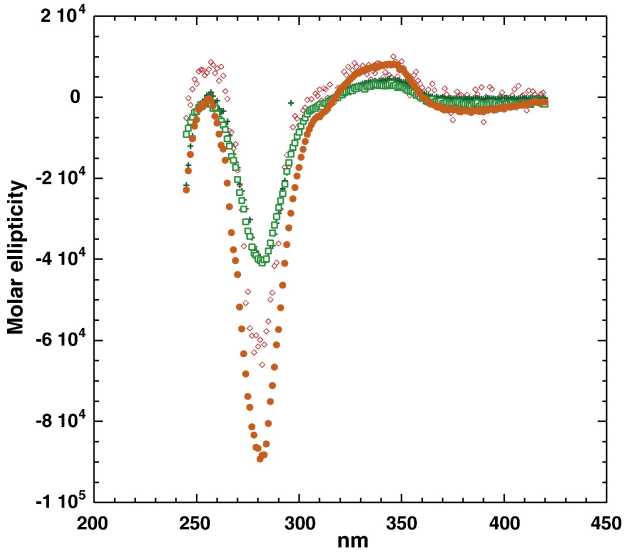

Fig. 5. Molar ellipticity curves for ANS bound to various mutants: (●) wild type I-FABP, (✧) W6Y, (❑) W82Y, (+) W6YW82Y.

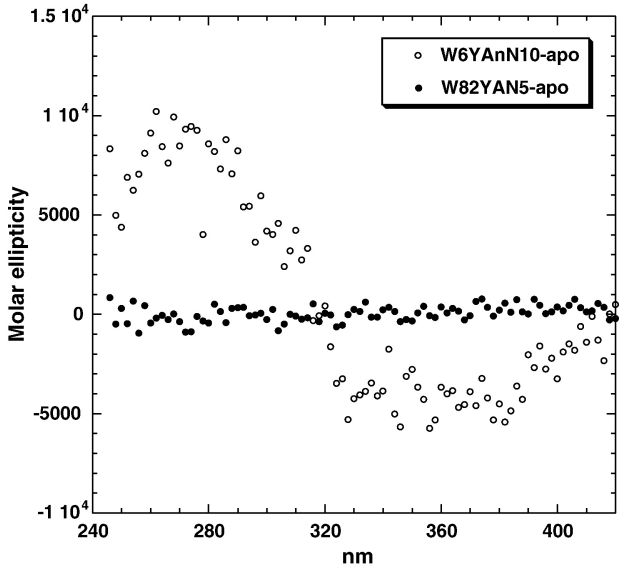

Fig. 7. Molar ellipticity of W82Y mutant plus AnN (●) minus that of protein alone (protein itself has a slight contribution, negligible in the case of ANS but noticeable in the case of AnN), and of AnN in mutant W6Yminus that of protein alone in (○).

explication for this behavior may be phenomena we invoke below, but the direct mechanisms we discussed in this report would not seem to be operable. Interestingly, Fig. 8 showing the CD in the near UV from aminonaphthalene sulfonate (AmNS) demonstrates that the *trp*-82 signal is unambiguously in the same direction as the ANS signal, despite there being no A/B transition to couple with. Moreover, the intensity is quite similar to the *near visible* intensity of the naphthalenic bands for AnN and ANS. It seems possible that the far from resonance interaction of trp L_a and L_b with naphthalene L_a and L_b of ANS and AnN are comparable, and possibly the reverse interaction for AmNS onto trp L_a and L_b is also similar (sign and intensity). The *near visible* CD in AmNS possibly vanishes because the two naphthalenic transitions for AmNS, which presumably have opposite signs (as do those of ANS and AnN), are substantially more overlapped in energy than the L_a and L_b transitions of either ANS or AnN.

We now turn to these far from resonant interactions which may well dominate the correlation between the strength of CD and local 'order parameter' [7].

3.1. Induced CD and order parameters

The 'A' transition of ANS was calculated (in II) to have an imaginary component. That is, once the $|A\rangle$ exciton was found and the $\mathbf{f}(A)$ energy distribution was created, it was seen that the

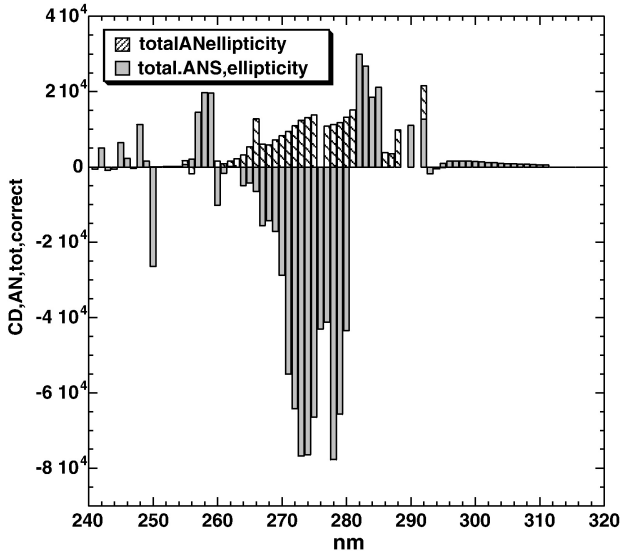

Fig. 6. Molar ellipticity *as calculated* for AnN and ANS for single trp interaction with *trp*-82 (thus comparable with the W6Y data)—shaded bar is the total CD calculated for ANS, hatched bar the total CD for AnN.

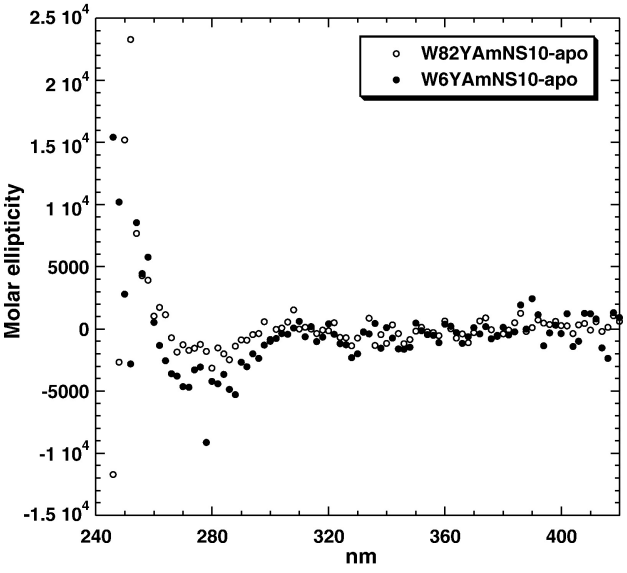

Fig. 8. Molar ellipticity of AmNS complex in W6Y (minus the protein itself) (●), that of AmNS complex with W82Y (○).

distribution, which is, to reiterate, the square of the excitonic wavefunction, dips into the negative domain. The 'absolute value' is still taken when used in an actual spectrum, so that the spectral representation is not itself ever negative. One can look at this imaginary component as due to the *rotation* of a charge about the direction of the electronic transition momentum—that is, a *twisted internal charge transfer* excitation. There would naturally be some CD associated with such a transition. However, in an isotropic environment, say in water solution, one sense of *twist* is just as likely as the opposite sense, and the net CD activity will be zero, as it must be for any molecule which has mirror image superposition symmetry, as does the dynamically averaged solution structure of ANS. But ANS *locked* into a specific conformation on a protein, as we mentioned in Introduction, cannot be superimposed with ANS locked into the opposite sense conformation—because of steric crowding at the binding site. Thus, because of the anisotropic environment, the *intrinsic* Cotton effect of ANS will become manifest. The environment selects one versus the other sense of twist. But as we saw, this contribution was not dominant for the FABP-bound anilinonaphthalenes.

This environmental selection effect can be generalized to other kinds of CD enhancement due to binding to a protein, and some of these additional effects are possibly operable in the case of I-FABP. It is commonly observed, for example (6), that solutions of (chiral) amino acids have, on a per-mole basis, far less CD activity than the same amino acid *residues* have in proteins, on a per-residue basis, and moreover that a presumably more fixed environment often yields a larger CD signal than a looser environment (e.g. native versus denatured proteins). We can look at this from the point of view of *local field* selection effects, rather than steric effects. Classically, an electromagnetic wave impinges on the protein. Since the polarizability tensor of the whole protein particle may not be isotropic, a net polarization may be induced in the protein, equivalent to the sum of all electric dipoles induced in the protein volume. These may well have a net orientation relative to a particular transition at a particular residue. If centered at a point distinct from that of the residue of interest, say, by a displacement $\mathbf{R}$, this net induced polarization $\mathbf{P}$ would generate a distributed magnetic dipole: $\mathbf{R}\times\mathbf{P}\varpi$, and hence could lead to induced CD:

$$\boldsymbol{\mu}\cdot\mathbf{R}\times\mathbf{P}\varpi \tag{11}$$

The induced polarization here depends on the correlation of induced dipoles at many different parts of the protein. Thus, it is likely to be affected by segmental motility, in the sense that a statistical average of all the protein molecules in solution may cause the net polarization to average to a small value. So this induced CD effect would probably be sensitive to structural 'order' parameters. There is some similarity in (11) to a semi-classical explanation of hyper- or hypochromicity, either of which are also often correlated to empirical 'order' parameters. Indeed, our two-quantum (quadrupole–dipole) formalism also has an analog in a novel two-quantum hyper(hypo)chromism mechanism as well: the idea is that the local field generated by one transition electric dipole called E_{ind} interacts with a second dipole by means of the polarizability of the second dipole, or $1/2\boldsymbol{\alpha}E_{\mathrm{ind}}^2$ where $\boldsymbol{\alpha}$ is the polarizability of the second residue. The whole additional transition probability then is proportional to (*cf.* (5a) (5b) (5c)):

$$[\boldsymbol{\mu}_1/(E-h\nu)]\{[3\mathbf{n}(\boldsymbol{\mu}_1\cdot\mathbf{n})-\boldsymbol{\mu}_1]/R^3\}\cdot\alpha\cdot\{[3\mathbf{n}(\boldsymbol{\mu}_1\cdot\mathbf{n})-\boldsymbol{\mu}_1]/R^3\}\boldsymbol{\mu}_2 \tag{12}$$

The two-quantum formalism adopted for our 'new' mechanism suggested to us, because of its similarity with hypochromism and Raman effects, the ideas we sketch above for more general CD inductive effects in proteins. Moreover, it is likely that just such effects as these may play a role in the near visible CD spectra observed for various aminonaphthalenes bound to I-FABP, in an energy regime far from resonance with any other transitions.

The 'quadrupole/induced gradient' mechanism itself may now be considered as a possible alternative in many proteins, especially where the ordinary distributed dipole coupling is thought to be small.

Acknowledgements

This work was supported by NIH grant GM34847 to Franklyn G. Prendergast, in whose laboratory this work was performed. Dr. Prendergast proposed and initiated the overall investigation of the photophysics of Intestinal Fatty Acid Binding Protein, both in the wild type and mutants, conducted by this laboratory.

Appendix A

We wish to find the eigenvalues of **M**2, or solve the determinant

$$\det\begin{Bmatrix} |H_{\mathrm{A}}-E & H_{\mathrm{Aa}} & H_{\mathrm{Ab}} & | \\ |H_{\mathrm{Aa}} & H_{\mathrm{a}}-E & 0 & | \\ |H_{\mathrm{Ab}} & 0 & H_{\mathrm{b}}-E & | \end{Bmatrix}$$

In practice, we solve the secular equation in terms of $E-W=X$, where $W=1/3$ Tr **M**2, or:

$$\begin{aligned} X^3 &+ X\{H_{\mathrm{A}}(H_{\mathrm{a}}+H_{\mathrm{b}})+H_{\mathrm{a}}H_{\mathrm{b}}-3W^2-H_{\mathrm{Aa}}^2-H_{\mathrm{Ab}}^2\} \\ &+ W[H_{\mathrm{A}}(H_{\mathrm{a}}+H_{\mathrm{b}})+H_{\mathrm{a}}H_{\mathrm{b}}]-2W^3-(H_{\mathrm{Aa}}^2+H_{\mathrm{Ab}}^2)W \\ &- H_{\mathrm{A}}H_{\mathrm{a}}H_{\mathrm{b}}+H_{\mathrm{Aa}}^2H_{\mathrm{b}}+H_{\mathrm{Ab}}^2H_{\mathrm{a}}=0 \end{aligned}$$

Calling the coefficient of X 'p' and the remainder 'q', we solve the cubic equation as follows: with $\omega=[(-q)^2/4-(p^3/27)]$, then a modulus *mod* defined by $mod^2=q^2/4+\omega^2$ and an angle θ by $\arctan\theta=\omega/\mathrm{mod}$ produces the three roots by $(mod)^{1/3}(2\cos(\theta/3))$; $(\mathrm{mod})^{1/3}(2\cos(\theta/3+2\pi/3))$; $(mod)^{1/3}(2\cos(\theta/3+4\pi/3))$. Taking these 'roots' and adding back 'W', dividing by the energy and differentiating, we have our new distributions $\mathbf{f}_0$, $\mathbf{f}_1$ and $\mathbf{f}_2$ for 'A' mixed with L_a and L_b, as well as for 'B' mixed with L_a and L_b (a separate matrix for 'A' and 'B'). Careful readers will note that we have now got *two* functions $|a,\mathrm{new}\rangle$ and $|b,\mathrm{new}\rangle$ which is not physically correct—we must in fact have only one of each. In other words, we *ought* to have solved the 4×4 matrix that includes the $\langle B|H|B\rangle$ and the off-diagonal terms containing $|B\rangle$, and then solved for the four actual eigenfunctions of the problem, instead of solving

two 3×3 matrices as we have done. Solving the 4×4 would have necessitated more complexity than we were willing to introduce at the time. Instead, we reasoned that, as long as the parts of the function $|a\rangle$ (and the function $|b\rangle$) that actually interact with the functions $|A\rangle$ and $|B\rangle$ have zero overlap, i.e. as long as these parts are completely independent, then a separation into two 3×3 matrices can be invoked. The 'double counting' of the $\langle a|H|a\rangle$ and $\langle b|H|b\rangle$ matrix elements is corrected for by dividing these terms implicitly by 2; thus, the actual matrix elements used in solving **M**1, or its equivalent with the function $|B\rangle$, are *half* the values of the ones given. This permits the sum of the traces of the two 3×3 matrices to equal the trace of the 4×4 matrix we thereby avoided solving. The off-diagonal terms $\langle A|H|b\rangle$, etc. appear in the two 3×3 matrices exactly as many times as in the 4×4 matrix, so it is unnecessary to correct them.

References

[1] E. Power, T. Thirunamachandran, Circular dichroism: a general theory based on quantum electrodynamics, J. Chem. Phys. 60 (9) (1974) 3695–3701.

[2] L. Rosenfeld, Quantenmechanische Theorie der natürlichen optischen Aktivität von Flüβigkeiten und Gasen, Z. Phys. 52 (1928) 161–174. Rosenfeld introduces an antisymmetric $\mathbf{rp}_{ij}$ tensor matrix element, evaluated under an electromagnetic wave with u_k directional component—which expression turns out to be the same thing as the orbital magnetic dipole element. However, if we take cognizance of the 'direction' imposed by the field gradient, we can contract an $\mathbf{rr}_{ij}$ (quadrupole) matrix instead, leaving the term involving the electric dipole of the second transition intact (or $\mathbf{p}_j$); the dipole moment matrix element of the 'assisting' transition inducing the field gradient. Then we recover our formula, within the context of two-quantum effects.

[3] P. Callis, ^1L_a and ^1L_b transitions of tryptophan, Methods Enzymol. 278 (1997) 113–150. Rosenfeld introduces an antisymmetric $\mathbf{rp}_{ij}$ tensor matrix element, evaluated under an electromagnetic wave with u_k directional component—which expression turns out to be the same thing as the orbital magnetic dipole element. However, if we take cognizance of the 'direction' imposed by the field gradient, we can contract an $\mathbf{rr}_{ij}$ (quadrupole) matrix instead, leaving the term involving the electric dipole of the second transition intact (or $\mathbf{p}_j$); the dipole moment matrix element of the 'assisting' transition inducing the field gradient. Then we recover our formula, within the context of two-quantum effects.

[4] W. Heitler, The Quantum Theory of Radiation, Oxford Univ. Pr., 1954, pp. 138–145.

[5] P.A.M. Dirac, The Principles of Quantum Mechanics, Oxford Univ. Pr., 1958, pp. 145–148.

[6] J. Sirangelo, C. Malmo, M. Casillo, G. Irace, Photochem. Photobiol. 76 (2002) 381–384.

[7] E.H. Strickland, Aromatic contributions to CD spectra in proteins, CRC Crit. Rev. Biochem. 2 (1974) 113–175.